Modelling and Simulation of Mechatronic Systems

Jonathan Smyth, Marvin Mouroum, Askhat Issakov, Cesar Gonzalez

Mai 2019

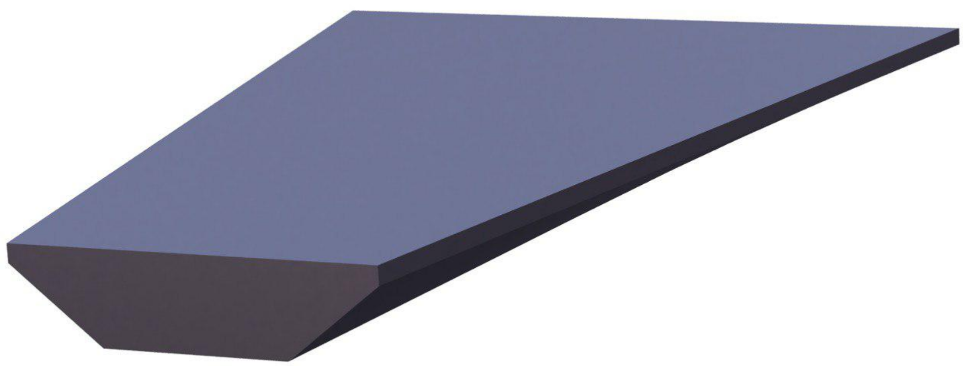

Kinematic Analysis of the AB Dynamic Driving Simulator

second milestone of course project

Contents

1 Abstract

The quality of the driving simulator depends on its ability to mimic actual driving behaviour in a vehicle. The driver will feel accelerations and rotations that will give him the impression to be in a vehicle. The kinematic model is the basis for the user experience of the driver. The following report explains the generation of the kinematic model and it's implementation in Maple. It analyses different kinematic behaviours, with 2 out of 3 fixed degrees of freedom. It appeared that the maximum rolling ability of the system depends on the width of the platform, the length of the sliding joint l_i and the length of the rotating rod r. A maximum theoretical roll of $\pm 10°$ is attainable with the estimated dimensions. The heave ranges from $0\,mm$ to $700\,mm$ in theory, however due to geometry constraints a value of $400\,mm$ to $500\,mm$ is feasible. The analysis of the position helped to verify of the picked dimension of the system. The velocity analysis will be used to verify the selection of actuators and the acceleration of the COM center of mass will be beneficial for evaluating the forces felt by the driver.

2 Introduction

The kinematic model of the driving simulator from AB Dynamic was approached in 2 dimensions. The platform is displayed in the $Y-Z$ plane, which represents the front view of the system (Figure:1).

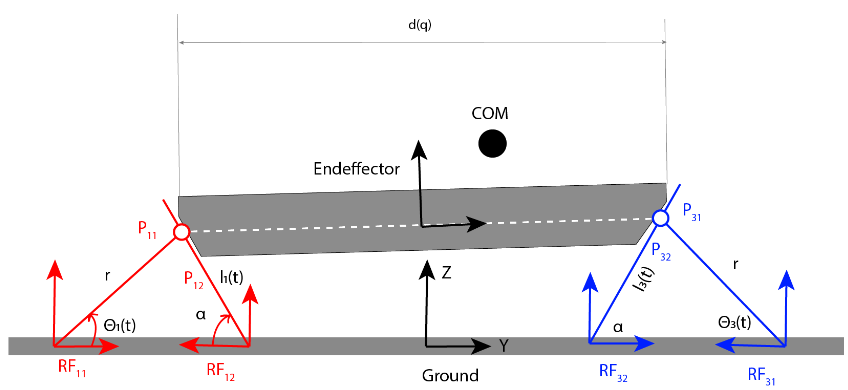

Figure 1: Sketch of the platform in 2D front view

3 Methodology

3.1 Analysis of Geometries

First looking at Figure 1, giving a cross sectional view in 2D ($Y - Z$ plane) of the platform and the actuating mechanism. The geometries of the system become apparent when breaking down the individual components. The system is comprised of a fixed length, d, modelled as the distance between P_{11} and P_{31}.

To begin with, this length will be used as a simplified version of the platform base, this is discussed in more detail in the next section. The value r, is fixed length of the actuating arms at q_{11} and q_{31}. The varying angles of θ_1 and θ_3. Finally the fixed angles of the sliders α, dictating the fixed gradient of the slope for the sliders. Overall, the geometric properties of the model clearly show us where it is constrained, this is discussed in next sections.

3.1.1 The Platform

For purposes of simplicity in this initial 2 D model, the platform is seen to be a line between P_{11} and P_{31}, with mid point half way between the 2 points. This approach is used to identify the range of positions the platform edges can exist and if they are suitable.

In reality and further into the development of the model the platform will be modelled as an elongated 3 D trapezoidal shape, the reason for this is to achieve more dynamic range of motion from a lesser work space. This shape allows the base depending on the configuration of the sliders to act like more than one shape at once. Currently the motion of the platform is limited to roll rotation along the X axis and translation along both the Z and the Y direction. As the development of the model is continued, this will be expanded to also take into consideration the yaw and pitch rotation, as well as the translation along X.

The platform is constrained in a few different places, the fixed length of d, constrains the platform as a function of the positions of P_{11} and P_{31} over time, which in turn are constrained by the length r, angle θ over time and fixed α.

3.1.2 Sliding Joints

When analyzing the sliders, it can be seen that from Figure 1, the mechanism can be viewed as a set of 2 dynamically changing triangle as a function of time. As the varying angles, θ_i change over time, so too does the configuration of the platform base.

Geometrically the sliders can only translate laterally in the Y plane (this is also true for the eventual 3 D model) with 1 degree of freedom, constrained by the length of the runners they exist in. The arms, can only transverse along the gradient of the legs $l_1(t)$ and $l_3(t)$ as a dependent of the angle α.These two properties have a direct impact on the ability of the platforms roll.

3.2 Creating Reference Frames

Figure 1 shows position and orientation of the system's reference frames. The left hand side is displayed in red as subgroup 1, whereas the right hand side is colored blue as subgroup 3. The notation is picked in a way that it's scale able to a 3 D solution, where the left hand site would be expanded by a subgroup 2 and the right hand side would receive an additional subgroup 4.
To be able to keep the angles positive and between 0° and 90°, RF_{12} and RF_{31} have been rotated around their Z axis by a factor of π. The translation along Y of the respective frame is given with the variable $q_{ij}(t)$.

$$RF_{11} = \begin{bmatrix} 1 & 0 & 0 & 0 \\ 0 & 1 & 0 & q_{11}(t) \\ 0 & 0 & 1 & 0 \\ 0 & 0 & 0 & 1 \end{bmatrix} RF_{31} = \begin{bmatrix} -1 & 0 & 0 & 0 \\ 0 & -1 & 0 & q_{31}(t) \\ 0 & 0 & 1 & 0 \\ 0 & 0 & 0 & 1 \end{bmatrix}$$
$$RF_{32} = \begin{bmatrix} 1 & 0 & 0 & 0 \\ 0 & 1 & 0 & q_{32}(t) \\ 0 & 0 & 1 & 0 \\ 0 & 0 & 0 & 1 \end{bmatrix} RF_{12} = \begin{bmatrix} -1 & 0 & 0 & 0 \\ 0 & -1 & 0 & q_{12}(t) \\ 0 & 0 & 1 & 0 \\ 0 & 0 & 0 & 1 \end{bmatrix}$$

3.3 Creating Points

The points P_{11} and P_{31} are computed by using their respective reference frame, rotate it by an angle θ_i and translate it along it's new Y axis by a positive value of r.
The points P_{12} and P_{32} are computed by using their respective reference frame, rotate it by an angle α and translate it along it's new Y axis by a positive value of $l_i(t)$.

$$P_{i1} = \begin{bmatrix} 0 \\ r\cos(\theta_i(t)) \\ r\sin(\theta_i(t)) \end{bmatrix}$$
$$P_{i2} = \begin{bmatrix} 0 \\ l_i(t)\cos(\alpha) \\ l_i(t)\sin(\alpha) \end{bmatrix}$$

Finally for creating the end effector E, a vector $\vec{V}$ is created that connects P_{11} and P_{31} (or alternatively P_{12} and P_{32}). $\vec{V}$ is devided by two and added to P_{11} (eq. 1). Given the roll constraint of the system of 16° (AB Dynamics

Brochure) the angle may be between $\pm 8°$. Because the angle may be negative, and is guaranteed to be within $[\pi,\pi]$, γ can be computed using eq.2.

$$E_{position} = P_{11} + \frac{\vec{V}}{2} \tag{1}$$

$$\gamma = \arctan(\vec{V}_Z, \vec{V}_Y) \tag{2}$$

3.4 Center of Mass

The center of mass of the platform depends on it's form, volume and mass as well as the mass and the position of the driver. The platform is symmetric along the $x-z$ plane and asymmetric along the $y-z$ plane. Figure 2 displays the platforms geometry. Regarding the overall weight of the system of 450 kg, the weight of the platform is estimated to be 300 kg. With the given shape, this forces the material of the platform to be some sort of fiber enforced thermoplastic. Using this material the payload of 500 kg is attainable and when manufactured in a light weight design will weigh around 300 kg. The driver is expected to weigh 80 kg. Because the drive is seated, the center of mass is assumed at the height of his chest. This would for an average height be approximately 30 cm above the sitting position. When adding 20 cm of seat height, the center of mass of the driver would appear 50 cm above the platforms top surface with a shift of 1/4 of the platforms overall width in the regarded section. The ratio between the masses is calculated in Eq. 3.4. Using the ratio the new COM can be computed to be at $[0.19, 0.12]m$ from the origin of the end effectors reference frame.

$$m_{ratio} = \frac{m_{driver}}{m_{platform}}$$

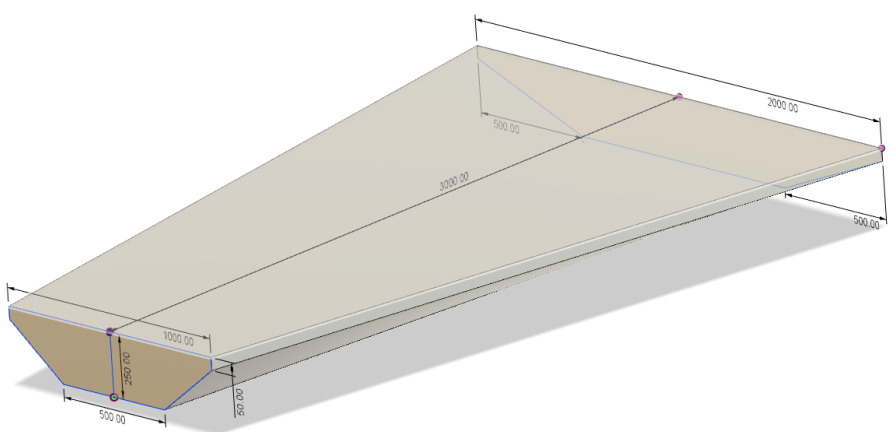

Figure 2: Geometry of the Platform

3.5 Establishing Constraints

The system currently is a 2 D problem with 3 DOF. However several separate entities have been evaluated and need to be put into relation to another. Creating the constrain equations is necessary to create the kinematic model of the system.

3.5.1 System Constraints

The system constraints are the constraints that create the kinematic model of the system.

$$\overline{P_{i1}P_{i2}} = \vec{0} \tag{3}$$

The points P_{i1} and P_{i2} are the same point

$$||\overline{P_{1j}P_{3j}}|| = d(q) \tag{4}$$

The points P_{1j} and P_{i2} have a rigid connection that depends on the X translation of the system. This translation can be neglected since this solution is focused on the 2D problem. However in regards to further investigation the distance between the points is given my a function $d(q)$, where q represents the translation of the platform along the end effectos x axis.

These constraints result in a set of system equations (eq.3.5.1). The distance represented by the function $d(q)$ is assumed to be $\frac{3}{2}r$.

$$\Phi_1 = \begin{bmatrix} \sqrt{\left(-l_1(t)\cos(\alpha) - l_3(t)\cos(\alpha) - q_{32}(t) + q_{12}(t)\right)^2 + \left(-l_1(t)\sin(\alpha) + l_3(t)\sin(\alpha)\right)^2} - 3/2\,r \\ -r\cos(\theta_1(t)) - l_1(t)\cos(\alpha) + q_{12}(t) - q_{11}(t) \\ -r\sin(\theta_1(t)) + l_1(t)\sin(\alpha) \\ -r\cos(\theta_3(t)) - l_3(t)\cos(\alpha) - q_{32}(t) + q_{31}(t) \\ -r\sin(\theta_3(t)) + l_3(t)\sin(\alpha) \end{bmatrix}$$

Given these constraints we can clearly identify 4 dependent variables in $l_1(t), l_3(2), \theta_1(t)$ and $\theta_3(t)$. However 4 variables remain represented by $q_{ij}(t)$. Given that it is a 2 D problem and there exist 5 constraint equations, one of the sliders will be dependent on the other three, leaving both 3 DOF and independent variables.

A further procedure would be to pick 3 independent coordinates of the q-set and solve Φ_1. However since the system is to be analyzed with 2 out of 3 DOF fixed, further constraints will be added before solving.

3.5.2 Position Constraints

The 2D problem has 3 possible independent movements in lateral translation (along Y), longitudinal translation (along Z) and rotation (along X). The lateral translation will be ignored, since it is trivial behaviour, kinematic solely dependent on the length of the systems slides. This leaves the "Heave" and the "Roll" as two an interesting subjects of analysis. To evaluate the roll of the system, the end effector position E will be held constant at an point P. The roll will be evaluated at an value of $h = 333mm$, meaning the end effector will be held stable $33cm$ above the ground.

$$P = \begin{bmatrix} 0 \\ h \end{bmatrix}$$

This will result in two more constraint equation, leaving only one independent parameter to adjust. However in order to analyzee the angle of rotation, an additional variable is introduced $\theta_2(t)$. This will represent the γ value and the resulting roll value of the system.

The new Φ vector consists of 8 equations, 8 dependent variables Q_D and one independent variable Q_I.

$$\Phi = \begin{bmatrix} \sqrt{\left(-l_1(t)\cos(\alpha) - l_3(t)\cos(\alpha) - q_{32}(t) + q_{12}(t)\right)^2 + \left(-l_1(t)\sin(\alpha) + l_3(t)\sin(\alpha)\right)^2} - 3/2\,r \\ -r\cos(\theta_1(t)) - l_1(t)\cos(\alpha) + q_{12}(t) - q_{11}(t) \\ -r\sin(\theta_1(t)) + l_1(t)\sin(\alpha) \\ -r\cos(\theta_3(t)) - l_3(t)\cos(\alpha) - q_{32}(t) + q_{31}(t) \\ -r\sin(\theta_3(t)) + l_3(t)\sin(\alpha) \\ 1/2\,r\cos(\theta_1(t)) - 1/2\,r\cos(\theta_3(t)) + 1/2\,q_{31}(t) + 1/2\,q_{11}(t) \\ 1/2\,r\left(\sin(\theta_1(t)) + \sin(\theta_3(t))\right) - h \\ \arctan\left(-r\left(\sin(\theta_1(t)) - \sin(\theta_3(t))\right), -r\cos(\theta_1(t)) - r\cos(\theta_3(t)) + q_{31}(t) - q_{11}(t)\right) - \theta_2(t) \end{bmatrix}$$

$$Q_D = \begin{bmatrix} \theta_1(t) \\ \theta_3(t) \\ \theta_2(t) \\ l_1(t) \\ l_3(t) \\ q_{12}(t) \\ q_{32}(t) \\ q_{31}(t) \end{bmatrix} Q_I = \begin{bmatrix} q_{11}(t) \end{bmatrix}$$

3.6 Solving the Constraint Equation

Φ can be solved by representing the dependent variables as equations of the independent variable $q_{11}(t)$. With the analytic solution it is possible to proceed to the analysis of the system.

The solution for the fixed rotation yields

$$\left[\begin{array}{c} \theta_1(t) = \arctan\left(1/12\sqrt{21 - 48\,(q_{11}(t))^2 - 72\,q_{11}(t)}\sqrt{3}, -q_{11}(t) - 3/4\right) \\ \theta_3(t) = \arctan\left(1/3\sqrt{21 - 48\,(q_{11}(t))^2 - 72\,q_{11}(t)}\sqrt{3}, \sqrt{16\,(q_{11}(t))^2 + 24\,q_{11}(t) + 9}\right) \\ \theta_2(t) = 0 \\ l_1(t) = 1/6\sqrt{21 - 48\,(q_{11}(t))^2 - 72\,q_{11}(t)} \\ l_3(t) = 1/6\sqrt{21 - 48\,(q_{11}(t))^2 - 72\,q_{11}(t)} \\ q_{12}(t) = 1/12\sqrt{21 - 48\,(q_{11}(t))^2 - 72\,q_{11}(t)} - 3/4 \\ q_{32}(t) = -1/12\sqrt{21 - 48\,(q_{11}(t))^2 - 72\,q_{11}(t)} + 3/4 \\ q_{31}(t) = 1/4\sqrt{16\,(q_{11}(t))^2 + 24\,q_{11}(t) + 9} + 3/4 \end{array}\right]$$

4 Results

4.1 Position Analysis

Initially, prior to the implementation of the model, the design specifications of the dimensions of the system were extrapolated from market research on pre-existing driving simulators.

However, post implementation and after initial testing with the the preconceived values yielded poor results indexed against the desired values that were needed. Initially a platform size of $2000x1800x1000mm$ was chosen. With those original values, the model was not able to satisfy the desired values for the specification. The width of $1800mm$ was too large to achieve the required rotational range for roll. Instead a more scientific approach was adopted. A relationship between the different dimension began to emerge, this is detailed below.

The first step to analyze the rotational properties of the model, was to constrain the system to fix the translation of the point end effector (Figure 1), in the Z and Y axis. This allowed the model to produce the bounded rotational freedom in the X axis (roll), enabling the construction of suitable real world dimensions for the simulator to achieve the desired functionality.

The conclusion was drawn that considerations for r, α, d,(Figure 1) and finally h, the height of the platform from the ground were needed to be taken into account when verifying the physical dimensions for the sliders and base width. Utilizing the researched values for the platform size gave a general starting point, which when modelled brought to light the importance of the other parameters mentioned above.

The process of modelling the different configurations of q_{11} (which is the independent coordinate of the system) allowed a reconstruction of how the the dependent coordinate will behave with respect to q_{11}. This was used to confirm that the constrained coordinates are within an ideal space for the desired behaviour of the model.

How the different configurations of position q_{11} effect the other points of interest in the model can be seen in Figure 3 below. These values were attained with the relationships between the variables as follows:

$$
\begin{aligned}
r &= 1000mm \\
d &= 6 * r/4 \\
\alpha &= \pi/3 \\
h &= r/3
\end{aligned}
$$

Using the above values, based on the kinematic model of the system, the model was able to produce a range of rotational motion in the X axis of +/-20°, this value was attained at a fixed height 333mm. However, given the fact the current system is being modelled as singular points in an analytic manner with no current considerations for real world physical dimensional constraints, this range of rotations is likely to decrease as further constraints are introduced in the model.

Consider how, for example the physical construction of the sliders and dimensions of the actual platform base will constrain further the available ranges of motion for the system. It can be said about the system that, at closer to the ground values for the end effector position, can indeed yield higher degrees of roll. This however, will need to be constrained by the physical dimensions of the other components of the system.

Figure 3: Plot of points, q_{11}, q_{12}, q_{31}, q_{32} and end effector

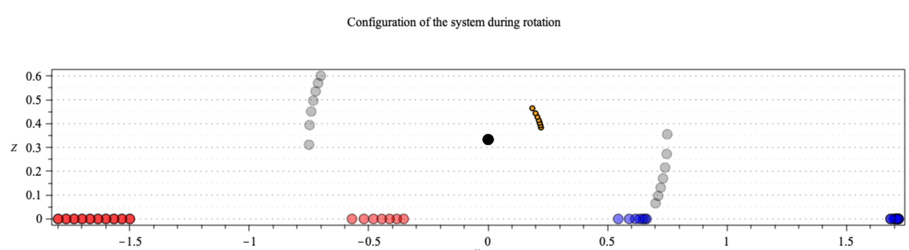

The red and blue dots represent to position of $q_{1,j}$ and $q_{3,j}$, respectively. The black dot represents the origin of the end effector and the gray dots represent the outer most edges of the platform geometry. The yellow dots represent the COM. A full rotation is displayed based on the independent movement of q_{11}. In order to have a full possible rotation the same movement needs to be redone with q_{31} since the two sides are symmetrical. The end effector's position was blocked and only rotation was allowed, moving q_{11} from -1.8 to -1.5m. This results in a possible rotation of the system of approximately 20°.

Figure 3 is a plot of the how the points, q_{12} (red), q_{31}(blue), q_{32}(blue), vary as the configuration of q_{11} changes. From Figure 3, the rotational the range of rotations for the platform can be computed.

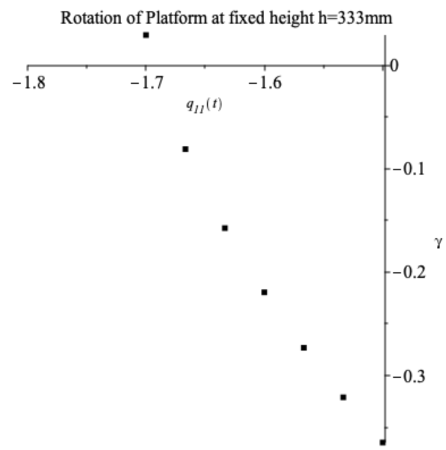

Figure 4: Rotational angle of the platform at configuration $q_{11}(t)$

The total amount of roll is therefore dependent on the platform width and the height of the end effector position and constraint by the ground and the minimal distance between the slider 12 and 32. It is also evident from Figure 4 that initial displacements result in a higher gradient. This could result in a loss in precision for small rotations.

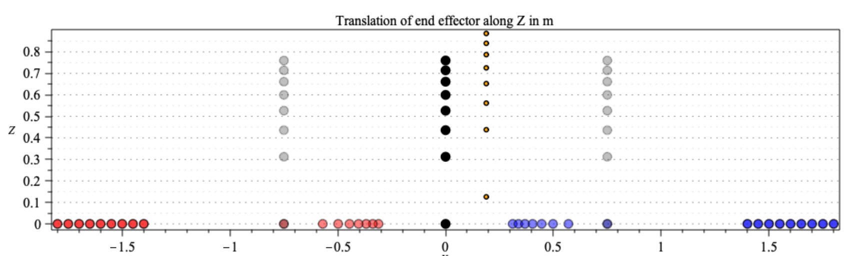

Figure 5: Plot of different configurations of q_{11} and COM

Fixating the rotation of the system, as well as lateral translation results in 8 possible solution, using the above presented set up. Theoretically a range

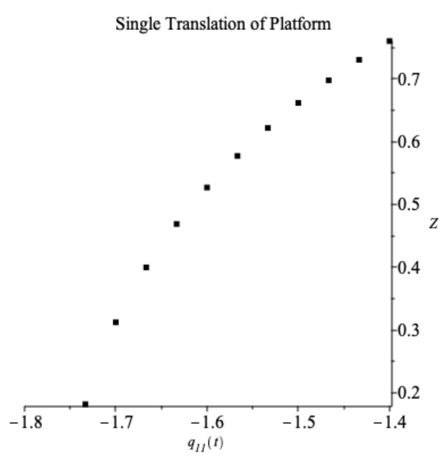

Figure 6: Plot of points, q_{11}, q_{12}, q_{31}, q_{32} and end effector.

from 0 to 750mm in heave is possible with the described setup. However physical constraints will make minimum and maximum positions less feasible. A reasonable range, regarding Figure 5 could be 400 to 500mm, according to the AB Dynamic brochure and a further benchmark review.

4.2 Velocity Analysis

The velocity analysis is giving insides of the attainable velocities of the system. The velocity of the end effector is evaluated (Figure 7) given the displacement of q_{11} from $-1.8\,m$ to $-1.4\,m$. Two components of the velocity of the end effector during roll are evaluated separately. Y component of the velocity decreases from $1\,\frac{m}{s}$ to 0. Z component of the velocity increases from $-1.2\,\frac{m}{s}$ to $-0.35\,\frac{m}{s}$.

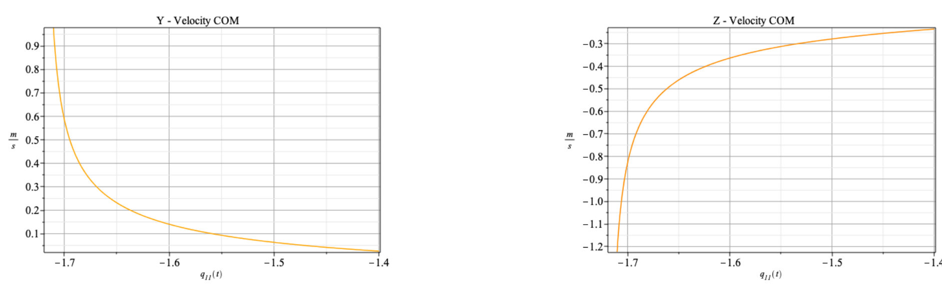

(a) Y component of angular velocity of the center of mass (COM)

(b) Z component of angular velocity of the center of mass (COM)

Figure 7: Velocity of the end effector

Current Specifications				
Motion	Degrees	Displacement	Velocity	Accel
Roll	$+/-20°$		1 m/s	$0.513m/s^2$
Heave		500mm		

Table 1: Current specification after the kinematic analysis

4.3 Acceleration Analysis

The acceleration analysis is giving insides of the attainable accelerations of the system. The acceleration of the end effector is evaluated (Figure 7) given the displacement of q_{11} from $-1.8\,m$ to $-1.4\,m$. Two components of the angular acceleration of the end effector are evaluated separately. Y component of the acceleration increases from $0.480\,\frac{m}{s^2}$ to $0.513\,\frac{m}{s^2}$ and then decreases until $0.508\,\frac{m}{s^2}$. Z component of the velocity increases from 0 to $-0.07\,\frac{m}{s^2}$.

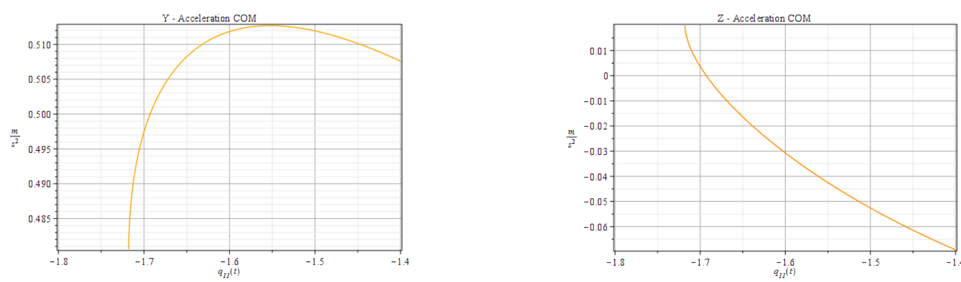

(a) Y component of angular acceleration of the center of mass (COM)

(b) Z component of angular acceleration of the center of mass (COM)

Figure 8: Acceleration of the end effector

4.4 Verified Model Specification

Table 1 shows the updated possible values given the model. Continuing with implementation of the model, the dimensions were chosen for the platform base of $3000x1000x250mm$ (max), due to the nature of the shape of the platform the width is variable as a function of the length(t). It can be seen in Figure 2 how the shapes dimensions are modelled.

The findings of the actual modelled values of the system based on the platform being at width $1500mm$: